PERGAMON

Computers & Geosciences 26 (2000) 167–175

COMPUTERS & GEOSCIENCES

The grid-spectral approach to 3-D geodynamo modelling ☆

P. Hejda [a,*], M. Reshetnyak [a, b]

[a] *Geophysical Institute, Academy of Science of the Czech Republic, Boční II c.p. 1401, 141 31 Prague 4, Czech Republic*
[b] *Institute of the Physics of the Earth, Russian Academy of Science, B. Gruzinskaya 10, Moscow, 123810 Russia*

Received 6 September 1998; received in revised form 15 June 1999; accepted 15 June 1999

Abstract

A 3-D kinematic geodynamo model in a sphere is considered. In contrast to the traditional spectral approach to the problem, a new grid-spectral method is proposed. The 3-D magnetic field and velocity field are resolved in the physical space for r- and θ-coordinates, whereas the sin- and cos-decomposition is applied to the φ-coordinate. The computer code was tested by free-decay solutions, as well as by comparison with the results reported by other authors. This work is the first step of a project to study 3-D inviscid geodynamo models. Published by Elsevier Science Ltd.

Keywords: Finite differences; Free decay modes; Asymmetric kinematic dynamo

1. Introduction

The geodynamo process of magnetic field generation occurs in the liquid spherical core of the Earth and is described by the 3-D magnetohydrodynamic (MHD) equations. Due to the complexity of these equations, the approach to the problem is usually numerical. The first models were kinematic, that is, with the fluid flow arbitrarily prescribed. The most frequently used method was already outlined in the pioneering paper of Bullard and Gellman (1954). It consists of decomposition of the magnetic and velocity fields into toroidal and poloidal parts and further expansion of the components in terms of spherical harmonics. The radial functions were either expanded in the series of base functions (for example Bessel functions, Chebyshev polynomials) or resolved on a grid. The advantage of this procedure is that the condition of non-divergence is satisfied automatically and the magnetic field can easily be fitted to an outer source-free potential field. The method was used in many dynamo simulations. Let us mention the 2-D kinematic models by Roberts (1972), 3-D kinematic dynamos by Gubbins (1973), Pekeris et al. (1973) or Dudley and James (1989), 2-D hydromagnetic models by Hollerbach et al. (1992), Hollerbach and Jones (1993) and also the advanced 3-D hydromagnetic dynamo models by Glatzmaier and Roberts (1995a, 1995b, 1996) and Kuang and Bloxham (1997).

A different approach to solve 2-D axisymmetrical models was adopted by Jepps (1975). It keeps the resolution into toroidal and poloidal parts but the resulting equations are approximated by a finite-difference scheme on a 2-D spherical grid in the meridional plane. The approach was widely applied to the axisymmetric hydrodynamic models in magnetostrophic ap-

☆ Code available at http://www.iamg.org/CGEditor/index.htm

* Corresponding author. Tel.: +420-2-6710-3339; fax: +420-2-7176-1549.

E-mail addresses: ph@ig.cas.cz (P. Hejda), rm@uipe.srcc.msu.su (M. Reshetnyak).

0098-3004/00/$ - see front matter Published by Elsevier Science Ltd.
PII: S0098-3004(99)00077-1

proximation (Braginsky, 1978; Braginsky and Roberts, 1987; Cupal and Hejda, 1989; Anufriev et al., 1995; Jault, 1995), in which the inertial and viscous forces were ignored in the bulk of the core and the velocity components were obtained by integration along the $\hat{z}$-axis. There are some indications that such models with marked vertical structures in the velocity field can be solved more easily by finite differences than by the spectral method. For example, the spectral solution of Hollerbach et al. (1992) fell into a chaotic regime just beyond the Ekman State breaking bifurcation, but the finite-difference calculations of the same model obtained independently by Anufriev et al. (1995) and Jault (1995) were able to follow further development of the solution.

Whereas the above-mentioned magnetostrophic models neglected the inner core effect, the method of solution for the axisymmetrical model with an inner core was developed by Anufriev (1994) and model calculations were done by Anufriev and Hejda (1998).

An entirely new method was developed by Nakajima and Roberts (1995). In this method, the grid points of one set of coordinates in the meridional plane lie on lines parallel to the axis of rotation and one curve of the other set coincides with the surface of the core. By this approach, the interpolation between spherical and cylindrical grids is avoided and, at the same time, the nonlocal condition on the magnetic field at the surface of the core can be easily implemented. The 3-D (asymmetric) magnetic field is represented by cylindrical components.

In the present paper we draw on our previous good experience with 2-D magnetostrophic models and keep the spherical coordinates. The 3-D magnetic and velocity fields are represented by three spherical components. The components are approximated by grid values for r- and θ-coordinates and sin- and cos- decomposition is then applied to the φ-variable. The method is tested by free decay modes as well as by comparison with kinematic dynamo models reported by other authors.

2. Basic equations

The generation of a geomagnetic field is described by the induction equation:

$$\frac{\partial \mathbf{B}}{\partial t} = \nabla \times (\mathbf{V} \times \mathbf{B}) - \nabla \times \eta \nabla \times \mathbf{B} \tag{1}$$

where $\mathbf{V}$ is the velocity field, which within the scope of the kinematic dynamo considered in this paper is the prescribed function of space coordinate $\boldsymbol{r}$ and time t, and η is the magnetic diffusivity which is usually constant. The additional conditions are the free divergence of the magnetic field, $\mathbf{B}$,

$$\nabla \cdot \mathbf{B} = 0 \tag{2}$$

and the incompressibility of the fluid,

$$\nabla \cdot \mathbf{V} = 0. \tag{3}$$

Vacuum boundary conditions for the magnetic field make up the complete problem.

It is well known that the case with $\mathbf{V} = 0$ can be solved analytically by using the toroidal-poloidal decomposition (Moffatt, 1978; Gubbins and Roberts, 1987; Backus et al., 1996; see also Section 6 of this paper for details). At the same time, the solutions (the so-called free decay modes) form a basis of the corresponding functional space. It can be seen that the magnetic field pertinent to the first poloidal mode is singular in the centre of the sphere. As it would cause problems in the numerical solution, we changed to the new variable $\mathbf{b} = r\mathbf{B}$ which is no longer singular in the centre.

Hereinafter we shall seek the solution in the following form:

$$\mathbf{b}(r,\theta,\varphi,t) = \begin{pmatrix} b_r \\ b_\theta \\ b_\varphi \end{pmatrix} = \sum_{m=0}^{M} \begin{pmatrix} b^c_{r_m} \\ b^c_{\theta_m} \\ b^c_{\varphi_m} \end{pmatrix} \cos m\varphi + \begin{pmatrix} b^s_{r_m} \\ b^s_{\theta_m} \\ b^s_{\varphi_m} \end{pmatrix} \sin m\varphi, \tag{4}$$

where b^c, b^s are the functions of r, θ and t and M is a truncation level. The substitution of Eq. (4) into Eq. (1) leads to the following equations for b_θ- and b_φ-components:

$$\frac{\partial b_\theta}{\partial t} = \nabla^2 b_\theta - \frac{b_\theta}{r^2 \sin^2\theta} + \frac{2}{r^2}\frac{\partial b_r}{\partial \theta} - \frac{2\cos\theta}{r^2\sin^2\theta}\frac{\partial b_\varphi}{\partial \varphi} + R_\theta, \tag{5a}$$

$$\frac{\partial b_\varphi}{\partial t} = \nabla^2 b_\varphi - \frac{b_\varphi}{r^2 \sin^2\theta} + \frac{2}{r^2\sin\theta}\frac{\partial b_r}{\partial \varphi} + \frac{2\cos\theta}{r^2\sin^2\theta}\frac{\partial b_\theta}{\partial \varphi} + R_\varphi. \tag{5b}$$

The b_r-component will be obtained from the nondivergence of the magnetic field Eq. (2) (see Section 4).

Eqs. (5a,b) lead to the following system of differential equations:

$$\frac{\partial b^c_{\theta_m}}{\partial t} = \nabla_1^2 b^c_{\theta_m} - \frac{1}{r^2}\frac{m^2}{\sin^2\theta} b^c_{\theta_m} - \frac{b^c_{\theta_m}}{r^2\sin^2\theta} + \frac{2}{r^2}\frac{\partial b^c_{r_m}}{\partial\theta} - \frac{2m}{r^2}\frac{\cos\theta}{\sin^2\theta} b^s_{\varphi_m} + R^c_{\theta_m}, \tag{6a}$$

$$\frac{\partial b^s_{\theta_m}}{\partial t} = \nabla_1^2 b^s_{\theta_m} - \frac{1}{r^2}\frac{m^2}{\sin^2\theta} b^s_{\theta_m} - \frac{b^s_{\theta_m}}{r^2\sin^2\theta} + \frac{2}{r^2}\frac{\partial b^s_{r_m}}{\partial\theta} + \frac{2m}{r^2}\frac{\cos\theta}{\sin^2\theta} b^c_{\varphi_m} + R^s_{\theta_m}, \tag{6b}$$

$$\frac{\partial b^c_{\varphi_m}}{\partial t} = \nabla_1^2 b^c_{\varphi_m} - \frac{1}{r^2}\frac{m^2}{\sin^2\theta} b^c_{\varphi_m} - \frac{b^c_{\varphi_m}}{r^2\sin^2\theta} + \frac{2m}{r^2\sin\theta} b^s_{r_m} + \frac{2m\cos\theta}{r^2\sin^2\theta} b^s_{\theta_m} + R^c_{\varphi_m}, \tag{6c}$$

$$\frac{\partial b^s_{\varphi_m}}{\partial t} = \nabla_1^2 b^s_{\varphi_m} - \frac{1}{r^2}\frac{m^2}{\sin^2\theta} b^s_{\varphi_m} - \frac{b^s_{\varphi_m}}{r^2\sin^2\theta} - \frac{2m}{r^2\sin\theta} b^c_{r_m} - \frac{2m\cos\theta}{r^2\sin^2\theta} b^c_{\theta_m} + R^s_{\varphi_m}, \tag{6d}$$

with $m = 0,\ldots M$,

$$\nabla^2 = \nabla_1^2 + \nabla_2^2, \tag{7}$$

$$\nabla_1^2 = \frac{\partial^2}{\partial r^2} + \frac{1}{r^2\sin\theta}\frac{\partial}{\partial\theta}\left(\sin\theta\frac{\partial}{\partial\theta}\right), \tag{8}$$

$$\nabla_2^2 = \frac{1}{r^2\sin^2\theta}\frac{\partial^2}{\partial\varphi^2}, \tag{9}$$

and R is the convective part of Eqs.(1) and (5a,b) decomposed in the form of Eq. (4):

$$\mathbf{R} = r(\nabla\times(\mathbf{V}\times\mathbf{b}/r)) = (\mathbf{b}\cdot\nabla)\mathbf{V} - r(\mathbf{V}\cdot\nabla)(\mathbf{b}/r). \tag{10}$$

The free divergence of the fields was used in the last equation. The following useful formulas for the system of spherical coordinates can be applied

$$(\mathbf{b}\cdot\nabla)\mathbf{V} = [\mathbf{b}\cdot\nabla V_r - (b_\theta V_\theta + b_\varphi V_\varphi)/r]\mathbf{e}_r + [\mathbf{b}\cdot\nabla V_\theta + (b_\theta V_r - \cot\theta\, b_\varphi V_\varphi)/r]\mathbf{e}_\theta + [\mathbf{b}\cdot\nabla V_\varphi + (b_\varphi V_r + \cot\theta\, b_\varphi V_\theta)/r]\mathbf{e}_\varphi, \tag{11a}$$

$$(\mathbf{V}\cdot\nabla)(\mathbf{b}/r) = [\mathbf{V}\cdot\nabla(b_r/r) - (V_\theta b_\theta + V_\varphi b_\varphi)/r]\mathbf{e}_r + [\mathbf{V}\cdot\nabla(b_\theta/r) + (V_\theta b_r - \cot\theta\, V_\varphi b_\varphi)/r]\mathbf{e}_\theta + [\mathbf{V}\cdot\nabla(b_\varphi/r) + (V_\varphi b_r + \cot\theta\, V_\varphi b_\theta)/r]\mathbf{e}_\varphi. \tag{11b}$$

Then

$$\begin{aligned}\mathbf{R} &= (\mathbf{b}\cdot\nabla)\mathbf{V} - r(\mathbf{V}\cdot\nabla)(\mathbf{b}/r)\\ &= [\mathbf{b}\cdot\nabla V_r - \mathbf{V}\cdot\nabla(b_r/r)]\mathbf{e}_r + [\mathbf{b}\cdot\nabla V_\theta - \mathbf{V}\cdot\nabla(b_\theta/r) + (b_\theta V_r - V_\theta b_r)/r]\mathbf{e}_\theta + [\mathbf{b}\cdot\nabla V_\varphi - \mathbf{V}\cdot\nabla(b_\varphi/r) + (b_\varphi V_r - V_\varphi b_r + \cot\theta(b_\varphi V_\theta - V_\varphi b_\theta)/r]\mathbf{e}_\varphi\\ &= [b_r\frac{\partial V_r}{\partial r} + \frac{b_\theta}{r}\frac{\partial V_r}{\partial\theta} + \frac{b_\varphi}{r\sin\theta}\frac{\partial V_r}{\partial\varphi} - rV_r\frac{\partial b_r/r}{\partial r} - \frac{V_\theta}{r}\frac{\partial b_r}{\partial\theta} - \frac{V_\varphi}{r\sin\theta}\frac{\partial b_r}{\partial\varphi}]\mathbf{e}_r + [b_r\frac{\partial V_\theta}{\partial r} + \frac{b_\theta}{r}\frac{\partial V_\theta}{\partial\theta} + \frac{b_\varphi}{r\sin\theta}\frac{\partial V_\theta}{\partial\varphi} - rV_r\frac{\partial b_\theta/r}{\partial r} - \frac{V_\theta}{r}\frac{\partial b_\theta}{\partial\theta} - \frac{V_\varphi}{r\sin\theta}\frac{\partial b_\theta}{\partial\varphi} + (b_\theta V_r - V_\theta b_r)/r]\mathbf{e}_\theta + [b_r\frac{\partial V_\varphi}{\partial r} + \frac{b_\theta}{r}\frac{\partial V_\varphi}{\partial\theta} + \frac{b_\varphi}{r\sin\theta}\frac{\partial V_\varphi}{\partial\varphi} - rV_r\frac{\partial b_\varphi/r}{\partial r} - \frac{V_\theta}{r}\frac{\partial b_\varphi}{\partial\theta} - \frac{V_\varphi}{r\sin\theta}\frac{\partial b_\varphi}{\partial\varphi} + (b_\varphi V_r - V_\varphi b_r + \cot\theta(b_\varphi V_\theta - V_\varphi b_\theta))/r]\mathbf{e}_\varphi.\end{aligned} \tag{12}$$

To obtain the explicit formulas for R^c, R^s selection rules similar to those of Bullard and Gellman (1954) for decomposing spherical function are required. Nevertheless, as the field is being expanded only in the φ-variable, our selection rules will be simpler.

3. Selection rules

The idea is to obtain equations for truncated Fourier series of the product of two Fourier series. Let

$$f = \sum_{m=0}^{M} f^c_m\cos m + f^s_m\sin m,$$
$$g = \sum_{k=0}^{M} g^c_k\cos k + g^s_k\sin k, \tag{13}$$

then

$$w = f\cdot g = \sum_{m=0}^{M} f_m^c \cos m \cdot \sum_{k=0}^{M} g_k^c \cos k + \sum_{m=0}^{M} f_m^c \cos m \cdot \sum_{k=0}^{M} g_k^s \sin k + \sum_{m=0}^{M} f_m^s \sin m \cdot \sum_{k=0}^{M} g_k^c \cos k + \sum_{m=0}^{M} f_m^s \sin m \cdot \sum_{k=0}^{M} g_k^s \sin k. \tag{14}$$

Equations for coefficients w^c, w^s expressed in terms of f^c, f^s, g^c, g^s are now required. After some simple algebra one arrives at:

$$w_0^c = \frac{1}{2}\left(f_0^c g_0^c + \sum_{m=0}^{M}\left[f_m^c g_m^c + f_m^s g_m^s\right]\right), \quad \text{for } 0 < p \le M:$$

$$w_p^c = \frac{1}{2}\left(\sum_{m=p}^{M}\left[f_m^c g_{m-p}^c + f_m^s g_{m-p}^s\right] + \sum_{m=0}^{M-p}\left[f_m^c g_{m+p}^c + f_m^s g_{m+p}^s\right] + \sum_{m=0}^{p}\left[f_m^c g_{p-m}^c - f_m^s g_{p-m}^s\right]\right), \tag{15}$$

$$w_0^s = 0, \quad \text{for } 0 < p \le M:$$

$$w_p^s = \frac{1}{2}\left(\sum_{m=0}^{p}\left[f_m^c g_{p-m}^s + f_m^s g_{p-m}^c\right] + \sum_{m=p}^{M}\left[-f_m^c g_{m-p}^s + f_m^s g_{m-p}^c\right] - \sum_{m=0}^{M-p}\left[-f_m^c g_{m+p}^s + f_m^s g_{m+p}^c\right]\right). \tag{16}$$

A similar analysis for $w = f\cdot g'$ leads to the following results:

$$w_0^c = \frac{1}{2}\sum_{m=0}^{M} m\left[f_m^c g_m^s - f_m^s g_m^c\right], \quad \text{for } 0 < p \le M:$$

$$w_p^c = \frac{1}{2}\left(\sum_{m=p}^{M}(m-p)\left[f_m^c g_{m-p}^s - f_m^s g_{m-p}^c\right] + \sum_{m=0}^{M-p}(m+p)\left[f_m^c g_{m+p}^s - f_m^s g_{m+p}^c\right] + \sum_{m=0}^{p}(p-m)\left[f_m^c g_{p-m}^s + f_m^s g_{p-m}^c\right]\right), \tag{17}$$

$$w_0^s = 0, \quad \text{for } 0 < p \le M:$$

$$w_p^s = \frac{1}{2}\left(\sum_{m=0}^{p}(p-m)\left[-f_m^c g_{p-m}^c + f_m^s g_{p-m}^s\right] + \sum_{m=p}^{M}(m-p)\left[f_m^c g_{m-p}^c + f_m^s g_{m-p}^s\right] - \sum_{m=0}^{M-p}(m+p)\left[f_m^c g_{m+p}^c + f_m^s g_{m+p}^s\right]\right). \tag{18}$$

Equations (15–18) were used to obtain coefficients R^c, R^s in Eq. (12).

4. Numerical scheme

In contrast to the toroidal–poloidal decomposition, where the non-divergence is automatically satisfied, in this formulation we must take account of it. It is well known that if the initial vector is non-divergent, the exact solution of Eq. (1) preserves this property. In the numerical solution there is the danger that the non-divergence of the solution will deteriorate due to numerical errors. It is, therefore, advisable to integrate Eq. (1) only for two components and compute the third component from the condition in Eq. (2). In contrast to Nakajima and Roberts (1995) who computed φ-component from Eq. (2), we have combined Eqs. (6a–d) with the following formulae for b_r:

$$b_r^{mc} = -\frac{1}{r\sin\theta}\int_0^r\left(\frac{\partial}{\partial\theta}(\sin\theta\, b_\theta^{cm}) + m b_\varphi^{sm}\right)\mathrm{d}r, \tag{19a}$$

$$b_r^{ms} = -\frac{1}{r\sin\theta}\int_0^r\left(\frac{\partial}{\partial\theta}(\sin\theta\, b_\theta^{sm}) + m b_\varphi^{cm}\right)\mathrm{d}r. \tag{19b}$$

In fact, the solution of the kinematic dynamo could be reduced to the eigenvalue problem. However, our computer code is the first step to the solution of the hydromagnetic (nonlinear) dynamo and that is why we have solved the parabolic problem. The finite-difference numerical scheme with central-difference approximation of the 2nd order of accuracy was applied on grid $\mathscr{G} = \{(r_i,\theta_j),\ i = 1,\ldots,N,\ j = 1,\ldots,K\}$, where $\theta_j = (j-1)h_\theta$, $h_\theta = \pi/(K-1)$ and the grid size in r may be regular or irregular. The diffusions (second-order derivative terms) in Eqs. (6a–d) were carried out implicitly, whereas the terms with the first-order derivatives were treated explicitly. The corresponding systems of linear equations were solved by the Gauss–

Seidel method. With the last r-layer the solution was obtained from the vacuum boundary conditions.

5. Vacuum boundary conditions

We make an usual assumption that the region of generation is surrounded by an insulator. The outer magnetic field may then be represented in the potential form

$$\mathbf{b} = -r\nabla U, \tag{20}$$

where U is the scalar potential of the field. The solution of the Eq. (20) has the form

$$U = \sum_{l=1}^{M}\sum_{m=0}^{l}(g_l^m \cos m\varphi + h_l^m \sin m\varphi) \\ P_l^m(\cos\theta)\left(\frac{1}{r}\right)^{l+1}, \tag{21}$$

where P_l^m are Legendre functions and g_l^m, h_l^m are Gauss coefficients which have to be determined.

The related equations for the field components at the surface of the sphere (Nth r-layer) have the form

$$\hat{b}_r = \sum_{l=1}^{M}\sum_{m=0}^{l}(\hat{g}_l^m \cos m\varphi + \hat{h}_l^m \sin m\varphi) \\ P_l^m(\cos\theta)(l+1), \\ \hat{b} = -\sum_{l=1}^{M}\sum_{m=0}^{l}(\hat{g}_l^m \cos m\varphi + \hat{h}_l^m \sin m\varphi)\frac{\mathrm{d}}{\mathrm{d}\vartheta} \\ P_l^m(\cos\vartheta), \\ \hat{b}_\varphi = \frac{1}{\sin\theta}\sum_{l=1}^{M}\sum_{m=0}^{l} m(\hat{g}_l^m \sin m\varphi - \hat{h}_l^m \cos m\varphi) \\ P_l^m(\cos\vartheta). \tag{22}$$

The simple form of the b_r-component in Eq. (22) encourage us to compute its first derivative in r as well:

$$\hat{b}_r' = -\frac{\partial}{\partial r}\frac{r\partial U}{\partial r} = -\sum_{l=1}^{M}\sum_{m=0}^{l}(\hat{g}_l^m \cos m\varphi + \hat{h}_l^m \sin m\varphi) \\ P_l^m(\cos\theta)(l+1)^2. \tag{23}$$

Conversely, this derivative may be expressed as follows

$$\frac{\hat{b}_r - b_r}{\delta r} = \sum_{l=1}^{M}\sum_{m=0}^{l}((\hat{g}_l^m - g_l^m)\cos m\varphi \\ + (\hat{h}_l^m - h_l^m)\sin m\varphi)P_l^m(\cos\theta)(l+1), \tag{24}$$

where the same decomposition as with the previous $(N-1)$th r-grid layer was used:

$$b_r = \sum_{l=1}^{M}\sum_{m=0}^{l}(g_l^m \cos m\varphi + h_l^m \sin m\varphi) \\ P_l^m(\cos\theta)(l+1). \tag{25}$$

We emphasize that, although the magnetic field is not potential in the $(N-1)$th layer, it can be decomposed into convergent series Eq. (25). Comparing Eq. (25) with Eq. (24) leads to the equations for the Gauss coefficients of the Nth layer:

$$\hat{g}_l^m = \frac{g_l^m}{(l+1)\delta r + 1}, \quad \hat{h}_l^m = \frac{h_l^m}{(l+1)\delta r + 1}. \tag{26}$$

Comparing Eq. (4) with Eq. (22) leads to the equations for g_l^m, h_l^m:

$$g_l^m = \frac{\int_0^\pi b_{r_m}^c P_l^m(\cos\vartheta)\sin\vartheta\,\mathrm{d}\vartheta}{(l+1)\int_{-1}^{+1} P_l^{m^2}(\mu)\mathrm{d}\mu}, \\ h_l^m = \frac{\int_0^\pi b_{r_m}^s P_l^m(\cos\vartheta)\sin\vartheta\,\mathrm{d}\vartheta}{(l+1)\int_{-1}^{+1} P_l^{m^2}(\mu)\mathrm{d}\mu}. \tag{27}$$

Here the Schmidt quasi-normalised form of the Legendre functions has been used:

$$P_l^0(\cos\vartheta) = P_{l,0}(\cos\vartheta), \\ P_l^m(\cos\vartheta) = \left[\frac{2(l-m)!}{(l+m)!}\right]^{1/2}\cdot P_{l,m}(\cos\vartheta), \\ \int_{-1}^{+1} P_l^{m^2}(\mu)\mathrm{d}\mu = \frac{4}{2l+1}, \quad \textit{for } m > 0, \\ \int_{-1}^{+1} P_l^{m^2}(\mu)\mathrm{d}\mu = \frac{2}{2l+1}, \quad \textit{for } m = 0. \tag{28}$$

Thus

$$\hat{g}_l^m = \frac{2l+1}{4(l+1)((l+1)\delta r + 1)}\int_0^\pi b_{r_m}^c P_l^m(\cos\vartheta)\sin\vartheta\,\mathrm{d}\vartheta, \\ \hat{h}_l^m = \frac{2l+1}{4(l+1)((l+1)\delta r + 1}\int_0^\pi b_{r_m}^s P_l^m(\cos\vartheta)\sin\vartheta\,\mathrm{d}\vartheta. \tag{29}$$

To obtain the boundary conditions for b_r-component in terms of coefficients $\hat{b}^c_{r_m}$, $\hat{b}^s_{r_m}$, they have to be expressed in terms of the Gauss coefficients $\hat{g}^m_l$, $\hat{h}^m_l$:

$$\sum_{m=0}^{M}\hat{b}^c_{r_m}\cos m\varphi+\hat{b}^s_{r_m}\sin m\varphi$$

$$=\sum_{l=1}^{M}\sum_{m=0}^{l}(\hat{g}^m_l\cos m\varphi+\hat{h}^m_l\sin m\varphi)P^m_l(\cos\vartheta)(l+1)$$

$$=\sum_{m=0}^{M}\sum_{l=m}^{M}(\hat{g}^m_l\cos m\varphi+\hat{h}^m_l\sin m\varphi)P^m_l(\cos\vartheta)(l+1). \quad (30)$$

Then

$$\hat{b}^c_{r_m}=\sum_{l=m}^{M}\hat{g}^m_l P^m_l(\cos\vartheta))(l+1),$$

$$\hat{b}^s_{r_m}=\sum_{l=m}^{M}\hat{h}^m_l P^m_l(\cos\vartheta)(l+1). \quad (31)$$

The substitution of Eq. (29) into Eq. (31) leads to

$$\hat{b}^c_{r_m}=\sum_{l=m}^{M}\frac{2l+1}{4((l+1)\delta r+1)}\int_0^{\pi}b^c_{r_m}P^m_l(\cos\vartheta)\sin\vartheta\,\mathrm{d}\vartheta \cdot P^m_l(\cos\vartheta),$$

$$\hat{b}^s_{r_m}=\sum_{l=m}^{M}\frac{2l+1}{4((l+1)\delta r+1)}\int_0^{\pi}b^s_{r_m}P^m_l(\cos\vartheta)\sin\vartheta\,\mathrm{d}\vartheta \cdot P^m_l(\cos\vartheta). \quad (32)$$

The same analysis for $\hat{b}_\vartheta$ and $\hat{b}_\varphi$ leads to

$$\hat{b}^c_{\vartheta_m}=-\sum_{l=m}^{M}\frac{2l+1}{4(l+1)((l+1)\delta r+1)}\int_0^{\pi}b^c_{r_m}P^m_l(\cos\vartheta)\sin\vartheta\,\mathrm{d}\vartheta \cdot\frac{\mathrm{d}}{\mathrm{d}\vartheta}P^m_l(\cos\vartheta),$$

$$\hat{b}^s_{\vartheta_m}=-\sum_{l=m}^{M}\frac{2l+1}{4(l+1)((l+1)\delta r+1)}\int_0^{\pi}b^s_{r_m}P^m_l(\cos\vartheta)\sin\vartheta\,\mathrm{d}\vartheta\cdot\frac{\mathrm{d}}{\mathrm{d}\vartheta}P^m_l(\cos\vartheta),$$

$$\hat{b}^c_{\varphi_m}=\frac{1}{\sin\vartheta}\sum_{l=m}^{M}m\frac{2l+1}{4(l+1)((l+1)\delta r+1)}\int_0^{\pi}b^c_{r_m}P^m_l(\cos\vartheta)\sin\vartheta\,\mathrm{d}\vartheta\cdot P^m_l(\cos\vartheta),$$

$$\hat{b}^s_{\varphi_m}=-\frac{1}{\sin\vartheta}\sum_{l=m}^{M}m\frac{2l+1}{4(l+1)((l+1)\delta r+1)}\int_0^{\pi}b^s_{r_m}P^m_l(\cos\vartheta)\sin\vartheta\,\mathrm{d}\vartheta\cdot P^m_l(\cos\vartheta). \quad (33)$$

Thus, since Eq. (2) is a first-order differential equation, we did not use the vacuum boundary condition, but integrated with respect to r from the centre of the inner core just to the last r-layer.

For convenience, to be able to compare our results with observations we used the quasi-Schmidt normalisation of Legendre functions. Gubbins' and Roberts' (1987)recurrent formulas were used to calculate them. The other reason of the applied normalisation is that the norm of the Legendre functions, defined by Eq. (28), does not include factorials which is an advantage in numerical simulations.

6. Test for free decay modes

The first test we performed was the test of induction Eq. (1) without fluid motions. Thus, only the diffusion of the magnetic field was taken into account. The analytical solution of Eq. (1) in a conductive sphere with $\mathbf{V}\equiv 0$ complemented by vacuum boundary conditions, is a series of eigen functions, the so-called free-decay modes:

$$\mathbf{b}^{decay}=e^{-k_l^2 t}\begin{pmatrix}(l+1)lj_l(k_l r)P^m_l(\cos\theta)\cos m\varphi,\\ -\dfrac{r}{\sin\theta}j_{l-1}(k_l r)mP^m_{l-1}(\cos\theta)\sin m\varphi+\cos m\varphi\dfrac{\partial}{\partial\theta}P^m_l(\cos\theta)(rj_{l-1}(k_l r)k_l-j_l(k_{l,m}r)),\\ -rj_{l-1}(k_l r)\cos m\varphi\dfrac{\partial}{\partial\theta}P^m_{l-1}(\cos\theta)-\dfrac{m\sin m\varphi}{\sin\theta}P^m_l(\cos\theta)(rj_{l-1}(k_l r)k_l-j_l(k_l r))\end{pmatrix}, \quad (34)$$

where j_l are a spherical Bessel functions and k_l are their roots obtained from the boundary conditions of the field (for details refer, e.g. to Moffatt, 1978; Gubbins and Roberts, 1987; Backus et al., 1996).

Here $l = 1,\ldots, \infty$. For $l = 1$ the terms with the $(l-1)$ index value for Bessel function must be omitted due to the absence of magnetic monopoles.

Since spherical coordinates are being used, one must formulate the boundary conditions not only on the surface of the sphere, but also at the centre ($r = 0$) and along the axis of rotation ($\theta = 0$, $\theta = \pi$). To do so we can make use of the fact that the free-decay modes form the basis of the space in which the solution is found.

Using Eq. (34) the additional boundary conditions in the centre of the sphere and at the axis of rotation $\hat{z}$ were applied.

Due to the asymptotics of spherical Bessel function j_l in the vicinity of the centre $j_l \sim r^l/[1\times 3\times\ldots\times(2l+1)]$, all components of $\mathbf{b}$ are zero for all l. As was mentioned above, the same asymptotics is singular for poloidal dipole components of $\mathbf{B}$. It caused the numerical instability in the original release of our computer code.

The boundary conditions along the axis of rotation were derived from the properties of Legendre functions. Thus, for the b_r-component in the vicinity of the axis of rotation, $b_r(\theta)\sim P_l^m$ and for $m \neq 0$ the b_r-component approaches zero. For $m = 0$, b_r is an even function on θ: $b_r \sim \cos^l\theta + 1$ and the first derivative with respect to θ is zero: $(\partial b_r/\partial\theta)|_{m=0} = 0$. For b_θ-component if $m = 0$, Eq. (34) yields $b_\theta \sim \sin\theta$ and $b_\theta \sim \sin^{m-1}\theta$ if $m > 1$, hence, the zero boundary condition applies to these values of m. For $m = 1$, $(\partial b_\theta/\partial\theta)|_{m=1} = 0$. Therefore, since the poloidal and toroidal terms of b_φ have the same structure with respect to θ to toroidal and poloidal terms of b_θ-component Eq. (34) respectively, the same conditions were applied to the b_φ-component.

In our test of the initial field distribution, we have used the particular single modes of this decomposition and compared the spatial distribution of the field during the computation as well as the magnitudes of the decay rates γ with analytical ones (γ_a). In our calculations γ was obtained as

$$\gamma = \frac{1}{2}\frac{\int |\dot{\mathbf{B}}|^2 d\mathbf{r}^3}{\int |\mathbf{B}|^2 d\mathbf{r}^3}.$$

We performed tests for all $1 \le l \le 6$ and $0 \le m \le l$. For Bessel functions we used the first root. In all cases the error has a tendency to decrease with increasing of number of points $(N\times K)$ as $1/(N\times K)$. To illustrate the convergence the corresponding maximal deviations of the magnetic field δB and decay rates $\delta\gamma = (\gamma - \gamma_a/\gamma_a)$ from analytical estimates for time moment $t = 0.01$ are presented in the Table 1.

Table 1
Convergence test for $l = 3$, $m = 0\ldots3$

m	0	1	2	3
$N\times K = 21\times 21$				
δB	−0.125	−0.068	−0.051	−0.021
$\delta\gamma$	−0.052	−0.042	−0.024	−0.008
$N\times K = 41\times 41$				
δB	−0.046	−0.016	−0.017	−0.006
$\delta\gamma$	−0.013	−0.010	−0.007	−0.002

7. Test on kinematic dynamo

In the general case, if $\mathbf{V} \neq 0$, the analytical solution of Eq. (1) with the prescribed arbitrary $\mathbf{V}$ is not known and the best way of checking a new numerical code is comparison with previous calculations. For this reason we chose the model of Gubbins (1973) (see also Dudley and James, 1989). To make our result compatible with theirs, we introduced some new definitions.

The decomposition of the prescribed velocity field in series of spherical functions leads to

$$\mathbf{V} = \mathbf{T} + \mathbf{S} = \sum_{l,m}(\mathbf{T}_l^m + \mathbf{S}_l^m), \tag{35}$$

where the following representations of the poloidal and toroidal fields are used:

$$\mathbf{V} = \mathbf{T} + \mathbf{S} = \nabla\times(T\mathbf{e}_r) + \nabla\times\nabla\times(S\mathbf{e}_r). \tag{36}$$

Then

$$T_{r,l}^m = 0, \quad T_{\theta,l}^m = \frac{T(r)}{r\sin\theta}\frac{\partial Y_{l,m}}{\partial\varphi}, \quad T_{\varphi,l}^m = -\frac{T(r)}{r}\frac{\partial Y_{l,m}}{\partial\theta}, \tag{37}$$

$$S_{r,l}^m = \frac{l(l+1)}{r^2}S(r)Y_{l,m,}, \quad S_{\theta,l}^m = -\frac{1}{r}\frac{\partial S(r)}{\partial r}\frac{\partial Y_{l,m}}{\partial\theta}, \quad S_{\varphi,l}^m = \frac{1}{r\sin\theta}\frac{\partial S(r)}{\partial r}\frac{\partial Y_{l,m}}{\partial\varphi}, \tag{38}$$

where $Y_{l,m}$ is a spherical function of order l and degree m with Neumann normalisation, see, e.g. Liley (1970).

Gubbins (1973) used the following form of the velocity field

$$\mathbf{V} = R_m(\mathbf{T}_2^0 + \epsilon\mathbf{S}_2^0), \tag{39}$$

with $\epsilon = 0.1$ and

$$T_2^0(r) = S_2^0(r) = -r^2 \sin(2\pi r)\tanh(2\pi(1-r)). \tag{40}$$

The explicit form of **V** reads

$$\mathbf{V} = \begin{pmatrix} -3\epsilon \sin(2\pi r)\tanh(2\pi(1-r))(3\cos^2\theta - 1) \\ \frac{3}{2}\epsilon[2\sin(2\pi r) + \tanh(2\pi(1-r)) + 2\pi r\cos(2\pi r)\tanh(2\pi(1-r)) - 2\pi r\sin(2\pi r)\cosh^{-2}(2\pi(1-r))]\sin 2\theta \\ -\frac{3}{2} r\sin(2\pi r)\tanh(2\pi(1-r))\sin 2\theta \end{pmatrix}. \tag{41}$$

The corresponding section of this field in equatorial and meridional planes are shown in Fig. 1 (upper row).

Dudley and James (1989) recalculated the results of Gubbins (1973) by solving the steady state of Eq. (1)

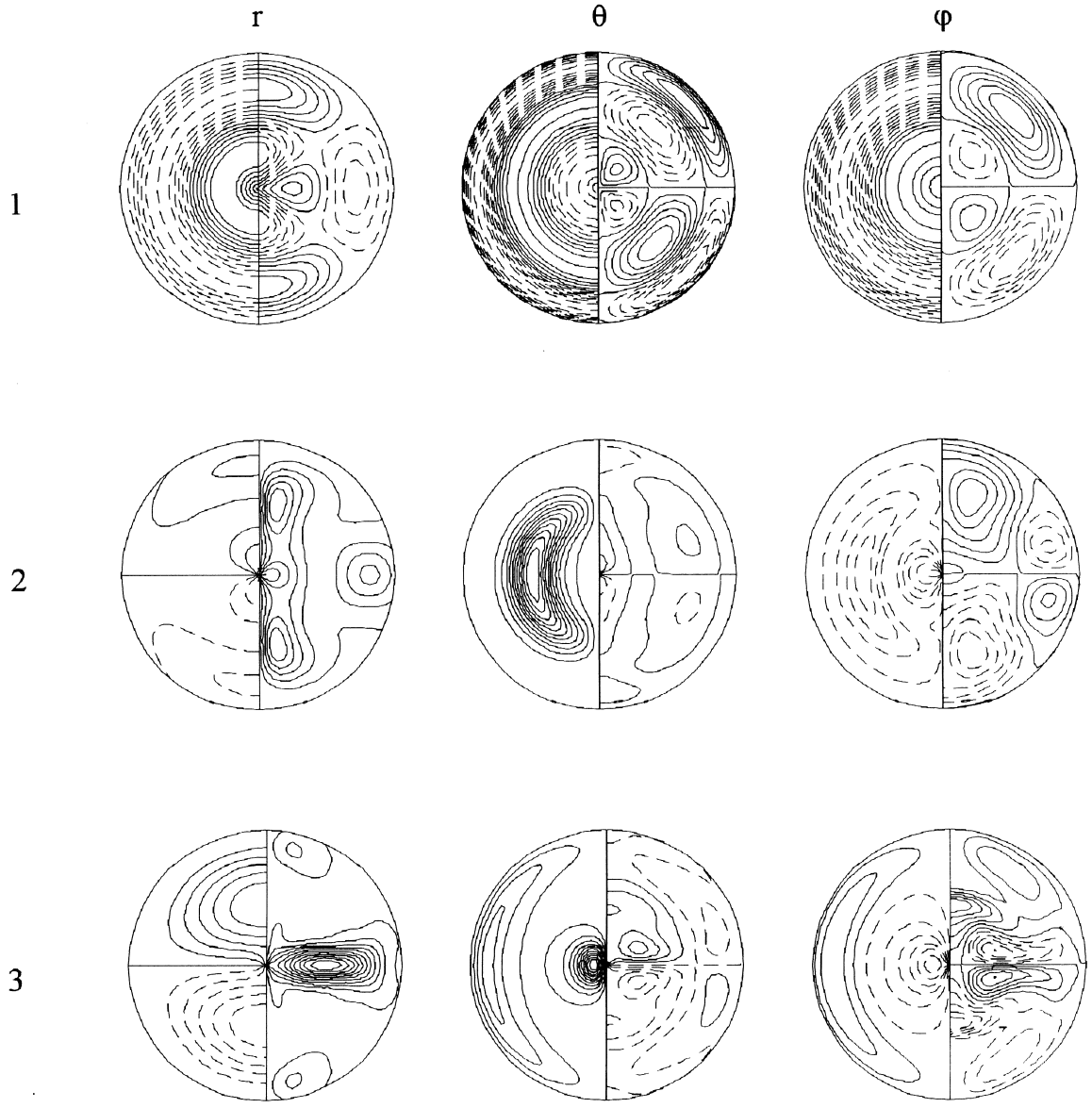

Fig. 1. Maps of Gubbins' model: r-, θ- and φ-components of velocity field (row 1), magnetic field for $R_m = 55$ (row 2) and magnetic field for $R_m = -95$ (row 3).

as an eigenvalue problem for R_m. The steady states $R_m = 54.7$ and -96.7, were accurately determined using 20 spherical functions and 100 grid points in r. We have found $R_m = 55.8$, -90.2 using 23×23 grid and $R_m = 54.8$, -93.5 using 45×45 grid. Whereas the agreement is excellent for positive threshold of generation, the less good agreement for the negative R_m is due to the more complex structure of the magnetic field (compare second and third rows of Fig. 1). To verify this result we made an additional integration using 89×89 grid. The resulting $R_m = -96.0$ indicates quadratic convergence to the value obtained by Dudley and James (1989).

8. Conclusions

In the modelling of the hydromagnetic dynamo one must pay particular attention to the correctness of the calculations. The best way of avoiding mistakes is to divide the computer code into several steps and check carefully every step. In harmony with these principles, the project of 3-D inviscid geodynamo modelling was started with the solution of the induction equation. In this first step we have developed the computer code of the model without the inner core. We have recovered, to good accuracy, the free decay modes as well as the solutions of the kinematic dynamo models of Dudley and James (1989). The method can be easily extended to the situation with the solid inner core, or modified to solutions of the scalar equation of thermal convection. This will be the subject of future work.

Acknowledgements

RM is grateful to the Geophysical Institute of the Czech Academy of Science in Prague for the support of his stay. The research was supported by the grant of RFBR 97-05-64797 and by the grant 205/97/0897 of the Grant Agency of the Czech Republic.

References

Anufriev, A.P., 1994. The influence of solid core on the Earth's hydrodynamics. Geophysical Astrophysical Fluid Dynamics 77, 15–25.

Anufriev, A.P., Cupal, I., Hejda, P., 1995. The weak Taylor state in an αω-dynamo. Geophysical Astrophysical Fluid Dynamics 79, 125–145.

Anufriev, A.P., Hejda, P., 1998. Effect of the magnetic field at the inner core boundary on the flow in the Earth's core. Physics of the Earth and Planetary Interiors 106, 19–30.

Backus, G., Parker, R., Constable, C., 1996. Foundations of Geomagnetism. Cambridge University Press, Cambridge, 369 pp.

Braginsky, S.I., 1978. Nearly axially symmetric model of the hydrodynamic dynamo of the Earth II. Geomagnetism and Aeronomy 18, 225–231.

Braginsky, S.I., Roberts, P.H., 1987. A model-Z geodynamo. Geophysical Astrophysical Fluid Dynamics 38, 327–349.

Bullard, E.C., Gellman, H., 1954. Homogeneous dynamos and terrestrial magnetism. Philosophical Transactions of the Royal Society of London A 247, 213–278.

Cupal, I., Hejda, P., 1989. On the computation of a model-Z with electromagnetic coremantle coupling. Geophysical Astrophysical Fluid Dynamics 49, 161–172.

Dudley, M.L., James, R.W., 1989. Time dependent kinematic dynamos with stationary flows. Proceedings of the Royal Society of London A 425, 407–429.

Glatzmaier, G.A., Roberts, P.H., 1995a. A threedimension convective dynamo solution with rotating and finitely conducting inner core and mantle. Physics of the Earth and Planetary Interiors 91, 63–75.

Glatzmaier, G.A., Roberts, P.H., 1995b. A threedimension selfconsistent computer simulation of a geomagnetic field reversal. Nature 377, 203–209.

Glatzmaier, G.A., Roberts, P.H., 1996. An anelastic evolutionary geodynamo simulation driven by compositional and thermal convection. Physica D 97, 81–94.

Gubbins, D., 1973. Numerical solutions of the kinematic dynamo problem. Philosophical Transactions of the Royal Society of London A 274, 493–521.

Gubbins, D., Roberts, P.H., 1987. Magnetohydrodynamics of the Earth's core. In: Jacobs, J.A. (Ed.), Geomagnetism, 2. Academic Press, London, 177 pp.

Hollerbach, R., Barenghi, C.F., Jones, C., 1992. Taylor constraint in a spherical αω-dynamo. Geophysical Astrophysical Fluid Dynamics 67, 3–25.

Hollerbach, R., Jones, C., 1993. A geodynamo model incorporating a finetely conducting inner core. Physics of the Earth and Planetary Interiors 75, 317–327.

Jault, D., 1995. Model Z by computation and Taylor's condition. Geophysical Astrophysical Fluid Dynamics 79, 99–124.

Jepps, S.A., 1975. Numerical models of hydromagnetic dynamos. Journal of Fluid Mechanics 67, 625–646.

Kuang, W., Bloxham, J., 1997. An Earthlike numerical dynamo model. Nature 389, 371–374.

Liley, F.E., 1970. On kinematic dynamos. Proceedings of the Royal Society of London 316, 153–167.

Moffatt, H.K., 1978. Foundations of Geomagnetism. Cambridge University Press, Cambridge, 343 pp.

Nakajima, T., Roberts, P.H., 1995. An application of mapping method to asymmetric kinematic dynamos. Physics of the Earth and Planetary Interiors 91, 53–61.

Pekeris, C.L., Accad, Y., Shkoller, B., 1973. Kinematic dynamos and the Earth's magnetic field. Proceedings of the Royal Society of London 275, 425–461.

Roberts, P.H., 1972. Kinematic dynamo models. Philosophical Transactions of the Royal Society of London A 272, 663–703.